Neo-Pleiades imagery for Posidonia oceanica mapping

Valerio Baiocchi
DICEA
Sapienza University of Rome
Rome, Italy
valerio.baiocchi@uniroma1.it

Alessandro Bosman
IGAG
CNR
Rome, Italy
alessandro.bosman@CNR.it

Flavia Cianfanelli
DICEA
Sapienza University of Rome
Rome, Italy
flavia.cianfanelli@uniroma1.it

Chiara Magurano
DICEA
Sapienza University of Rome
Rome, Italy
c.magurano@gmail.com

2025 IEEE 12th International Workshop on Metrology for AeroSpace (MetroAeroSpace) | 979-8-3315-0152-5/25/$31.00 ©2025 IEEE | DOI: 10.1109/MetroAeroSpace64938.2025.11114417

***Abstract*— *Posidonia oceanica* is an endemic plant in the Mediterranean whose presence depends on numerous natural and anthropic factors, which determine its irregular distribution throughout the basin. This makes it necessary to study the conditions that favour or limit the proliferation of *P. oceanica* and to adopt precise tools and mapping methods to monitor its health. Data obtained from remote sensing techniques require processing to prepare the images for possible analysis. The orthorectification process is a fundamental step in this image pre-processing phase. In this work, the application of both Object-Based Analysis and Pixel-Based Recognition classification methods was tested in order to isolate areas containing *Posidonia oceanica* in the image. The objective was to evaluate some of the most suitable mapping methods to provide accurate and repeatable data useful for the conservation of Posidonia meadows and the protection of the Mediterranean ecosystem. The results of the experimental work on orthorectification and *Posidonia oceanica* extraction methods are presented for a specific area of Sardinia (Italy).**

Keywords—Neo-Pleiades, Posidonia Oceanica, Sardinia, Orthorectification, object oriented, pixel based

I. Introduction

Posidonia oceanica (Linnaeus) Delile (from now on *P. oceanica*) is a marine flowering plant endemic to the Mediterranean Sea. As a flowering plant, it is capable of photosynthesis and possesses a system of roots, leaves, and fruits. *P. oceanica* plays a crucial role in coastal ecosystems, and the regression of its meadows has serious consequences for both the environment and human activities. Therefore, it is essential to study its biology, ecology, geographical distribution, as well as the threats it faces and the importance of its conservation.

Contrary to what its name might suggest, the meadows of *P. oceanica* are found along the coasts of the Mediterranean Sea, extending from the strait of Gibraltar to the coasts of Turkey and from the northern coasts of Africa to the Adriatic, occupying the continental shelf from shallow waters down to depths of 40-50 meters [1]. Its presence in these waters is far from uniform. The meadows develop under specific environmental conditions characterized by high water transparency, stable salinity levels, and a depth that allows for good light penetration. The impact of human activities, such as pollution, urban development, and maritime traffic, has contributed to a significant reduction and fragmentation of these meadows, compromising their ability to regenerate and thrive in certain areas [2][3].

Ecologically, their role extends well beyond merely providing habitat; they also actively contribute to water quality by absorbing nutrients. However, their most significant characteristic that has garnered particular interest in recent years is their function as blue carbon reservoirs, storing carbon dioxide in sediments and thereby reducing greenhouse gas concentrations in the atmosphere, which mitigates the effects of climate change [4]. Additionally, *P. oceanica* meadows protect coastlines from erosion caused by wave action [5].

The influence of human activities on marine ecosystems is a central theme in understanding the threats faced by this species. The meadows of *P. oceanica* span all Mediterranean coasts, covering approximately 2% of the submerged area [6]. In Italy, they are found in both the Tyrrhenian and Adriatic Seas, surrounding the islands of Sicily and Sardinia. Over the past 50 years, the population of *P. oceanica* has declined by 34%. In the north-western sector of the Mediterranean, which includes Liguria, the loss reaches 56% [7]. The habitat of *P. oceanica* extends from 0.5 to 40 meters in the sublittoral zones of the Mediterranean. In highly oligotrophic waters, it can reach depths of up to 50 meters, creating extensive and productive meadows. The optimal temperature for the growth of *P. oceanica* is around 20°C. Higher water temperatures, especially during marine heatwaves, can lead to decreased dissolved oxygen levels, negatively impacting the health of the meadows [8].

Given the aforementioned points, it is evident that monitoring *P. oceanica* meadows and developing various strategies to enhance monitoring efficiency is a topic of lively scientific debate. The tools typically employed for mapping underwater meadows are diverse and include established technologies such as aerial photography, side-scan sonar, and multibeam echosounders. In recent years, effective mapping increasingly relies on optical technologies, including satellite, aerial, and drone (UAV) remote sensing [9]. These methodologies are often integrated with laser techniques, such as LiDAR (Light Detection and Ranging), to enrich the available data with bathymetric components. In this study, remote sensing techniques were specifically applied to map *P.*

Authorized licensed use limited to: Universita degli Studi di Roma La Sapienza. Downloaded on December 11,2025 at 10:54:23 UTC from IEEE Xplore. Restrictions apply.

oceanica meadows, assess their health status, and analyse changes over time. Following data acquisition, geometric and thematic processing is required to accurately map the environmental features [10]. The data processing approach varies depending on the instrument used and the type of data provided by different suppliers, who may choose to release data at varying levels of rawness [11,12, 13 and 14].

For instance, in the study by [15], the collected data originated from Sentinel-1 and Sentinel-2 satellite surveys conducted over the Balearic and Maltese Islands in 2021. In contrast, this study utilizes two Neo-Pleiades images of the eastern coast of the Italian island of Sardinia. Initially, different techniques were employed for orthorectification using the Rational Polynomial Coefficient (RPC) model, incorporating Ground Control Points (GCPs) and Check Points (CPs) to separately evaluate precision and accuracy.

In this case, the orthorectification of the satellite image primarily concerns the submerged portion of the image, presenting two main challenges: the lack of available GCPs and the difficulty of performing geometric corrections due to the combined effects of water depth and refraction. Finally, we present the preliminary results of classification attempts for *P. oceanica* meadows using both pixel-based and object-oriented techniques.

II. Materials and Methods

This study involves the orthorectification and classification of satellite images acquired by the Neo-Pleiades constellation. The two images used are portions of raw acquisitions, captured on 27/11/2021 at 10:15 GMT and 02/01/2022 at 10:33 GMT. The Neo-Pleiades constellation follows a sun-synchronous orbit, ensuring that the satellites pass over the same location at the same time each day. This guarantees consistent illumination levels for images acquired over the same area.

As an Earth observation constellation, Neo-Pleiades operates in a low Earth orbit at an altitude of 620 km, enabling a very high nominal spatial resolution (30 cm for the panchromatic band and 1.2 m for the other spectral bands). Moreover, its near-polar orbit allows the satellites to partially cover the poles and traverse almost all terrestrial latitudes, achieving near-global coverage. Each satellite completes an orbit around the Earth in just 97.2 minutes, with a short revisit time that enables it to pass over the same point on the Earth's surface twice a day. The repetition cycle is 26 days, meaning the satellite will revisit the same area with the same observation geometry after this period. The satellite's swath width, or the across-track acquisition width, is 14 km. Launched in 2021, the constellation's satellites have an expected lifespan of 10 years.

Neo-Pleiades operates across multiple spectral bands:

- Panchromatic (450–800 nm)
- Deep blue (400–450 nm)
- Blue (450–520 nm)
- Green (530–590 nm)
- Red (620–690 nm)
- Red edge (700–750 nm)
- Near infrared (770–880 nm)

The two acquisitions presented here focus on a section of the northern coast of Sardinia, specifically the easternmost part of the Sassari province, between Golfo Aranci and Capo Ceraso.

To support the satellite data, additional datasets were obtained from the official Geo website of the Sardinia Region. These include a 1 m resolution Digital Terrain Model (DTM) derived from LiDAR data (where each pixel measures 1 m in both directions) and a 1:2000 scale Regional Technical Map (CTR) from the geographic database of urban centres and inhabited areas in Sardinia (DBGT_CU).

Regarding the bathymetric component, since no high-resolution bathymetric model is available through open-source platforms, contour lines were derived from a nautical chart provided by the Italian Hydrographic Institute (IIM).

The images were first imported into QGIS (v. 3.28) to extract the coordinates of approximately one hundred points, which were later used as GCPs and CPs for the orthorectification process, then carried out in PCI Catalyst (v. 2223.0.0). The first images to be orthorectified were the panchromatic ones. Subsequently, the multispectral images were orthorectified after undergoing a pansharpening process, using the same GCPs and CPs as those employed for the panchromatic images. The pansharpening process was performed using the dedicated module provided by the PCI Catalyst software.

For the multispectral images without pansharpening, an image coordinate conversion was performed to enable the use of the same GCPs and CPs.

III. RESULTS AND DISCUSSION

The previously described processes resulted in a total of 12 orthorectified satellite images. For each of the two years (2021 and 2022), the multispectral, panchromatic, and pansharpened images were orthorectified both with and without bathymetric correction.

To assess the accuracy of the images, it is essential to analyse the values obtained for the CPs. The orthorectification process ultimately employed approximately 80 GCPs and 20 CPs. The CP errors (ranging between 30 and 40 cm on average) are higher than those of the Ground Control Points (25–30 cm), as is typically observed. This discrepancy arises because the image is constrained by the GCPs, whereas the CPs serve as independent validation points (Tab. 1).

The CPs were randomly selected within the image (Fig. 1) and do not directly contribute to the estimation of the correction model.

Considering that the panchromatic images have a spatial resolution of 30 cm, the obtained errors fall within an acceptable range, as they are close to this value for both panchromatic and multispectral images. Interestingly, as observed in previous experiments, in Neo-Pleiades images orthorectified using RPC models, the elevation residuals on GCPs are lower than the planimetric residuals. This behaviour may be attributed to the relatively small elevation variation in the study area.

Authorized licensed use limited to: Universita degli Studi di Roma La Sapienza. Downloaded on December 11,2025 at 10:54:23 UTC from IEEE Xplore. Restrictions apply.

2021 Multispectral Image (ground units)			
	X RMS	Y RMS	Z RMS
GCP	0.268	0.242	0.097
CP	0.363	0.463	0.184

2022 Multispectral Image (ground units)			
	X RMS	Y RMS	Z RMS
GCP	0.24	0.277	0.13
CP	0.335	0.462	0.179

2021 Pansharpened Image (ground units)			
	X RMS	Y RMS	Z RMS
GCP	0.272	0.245	0.098
CP	0.362	0.462	0.184

2022 Pansharpened Image (ground units)			
	X RMS	Y RMS	Z RMS
GCP	0.244	0.281	0.132
CP	0.335	0.461	0.179

Table 1. Total residual errors expressed in ground units for the multispectral and the pansharpened images.

A well-known systematic difference exists between residuals in the North and East directions. Specifically, the accuracy of the X (East) coordinate is higher than that of the Y (North) coordinate.

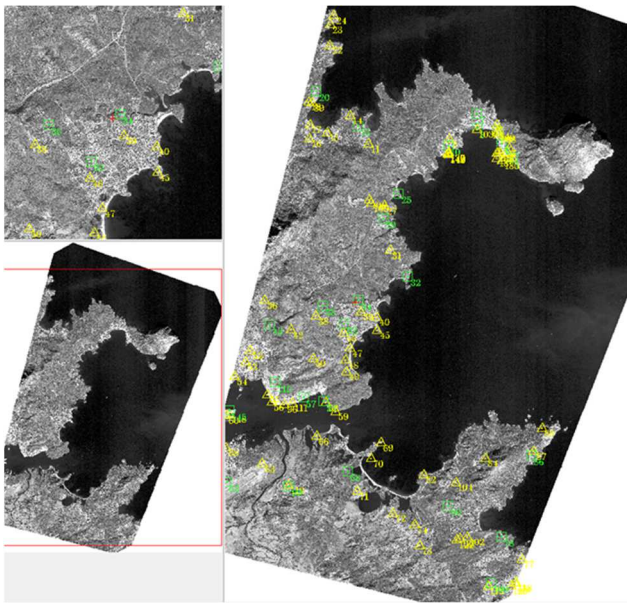

Fig. 1. Panchromatic image of 2021. Ground Control Points are shown in yellow, and Check Points in green

This is due to the satellite's pushbroom acquisition mode, in which the sensor captures an entire swath of terrain in a single instance along the direction orthogonal to the satellite's motion. The East coordinate is therefore acquired perpendicularly to the satellite's trajectory, making it more stable due to its geometrically "rigid" nature, which is less prone to temporal variations. In contrast, the North coordinate is influenced by the satellite's movement along its orbit, as well as by the stability of the platform and its navigation systems during acquisition. Since the image is progressively constructed as the satellite moves, minor instabilities in flight or data recording can introduce greater uncertainties in this direction [16]. In the latter case, in terms of orthorectification accuracy, it is currently not possible to rigorously assess the effect, as the ground control points (GCPs) and check points (CPs) used for orthorectification were measured on land, while no accurately measured control points are available on the seafloor. However, the effect of bathymetry can be observed with a difference in the shape and position of the seabed and consequently also the *P. oceanica* meadows. This shows how the effect of seabed depth cannot be neglected (Fig.2).

Fig. 2. Orthorectified pansharpened image of 2021 without bathymetric correction (top) and with bathymetric correction (bottom). The effect of using bathymetry shifts and changes the shape of the seabed

Following the application of pixel-based and object-oriented algorithms, it was possible to measure the total

Authorized licensed use limited to: Universita degli Studi di Roma La Sapienza. Downloaded on December 11,2025 at 10:54:23 UTC from IEEE Xplore. Restrictions apply.

coverage area of *P. oceanica* meadows. Only the orthorectified multispectral image from 2021 was imported into eCognition Essential (v. 10.4) to explore the potential for image classification. After initially masking out the land area, the classification was performed on the marine portion of the image. A pixel-based classification approach was applied, distinguishing between *P. oceanica* and open water using the MCARI index, as used in [17]. It is worth noting that, although the MCARI index values were negative underwater, they consistently fell within a distinct range (between -4 and -7) where *P. oceanica* could be identified, as confirmed through visual inspection. The object-based classification was performed by segmenting the marine area using specific parameters of shape (0.1), compactness (0.4), and scale (5) which enabled the software to delineate units closely following the natural contours of *P. oceanica* meadows on the seabed. The segmented units were subsequently classified as either water or *P. oceanica* based on their MCARI values.

The software then provided the meadow coverage area in pixels, requiring a conversion to square meters based on the spatial resolution of the images used (1.2 m).

The area calculations revealed a significant difference (1.4 km²) between the values obtained using the pixel-based (fig. 3) and object-based algorithms (fig.4) in the multispectral image without bathymetric correction.

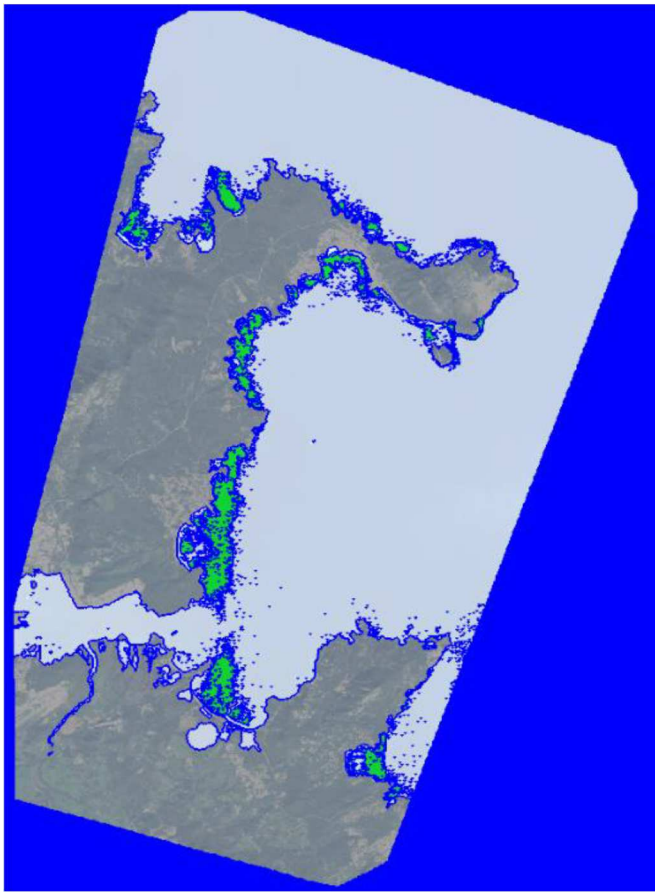

Fig. 3. Result of pixel based classification of the multispectral image of the year 2021 with bathymetric correction. In dark grey the land, in light grey the sea, in green the *P. oceanica.*

This discrepancy may be partially attributed to differences in the segmentation process of the marine surface between the two algorithms, as they employed different scale parameters. Notably, when classifying the same image with bathymetric correction, this difference was notably reduced (0.2 km^2).

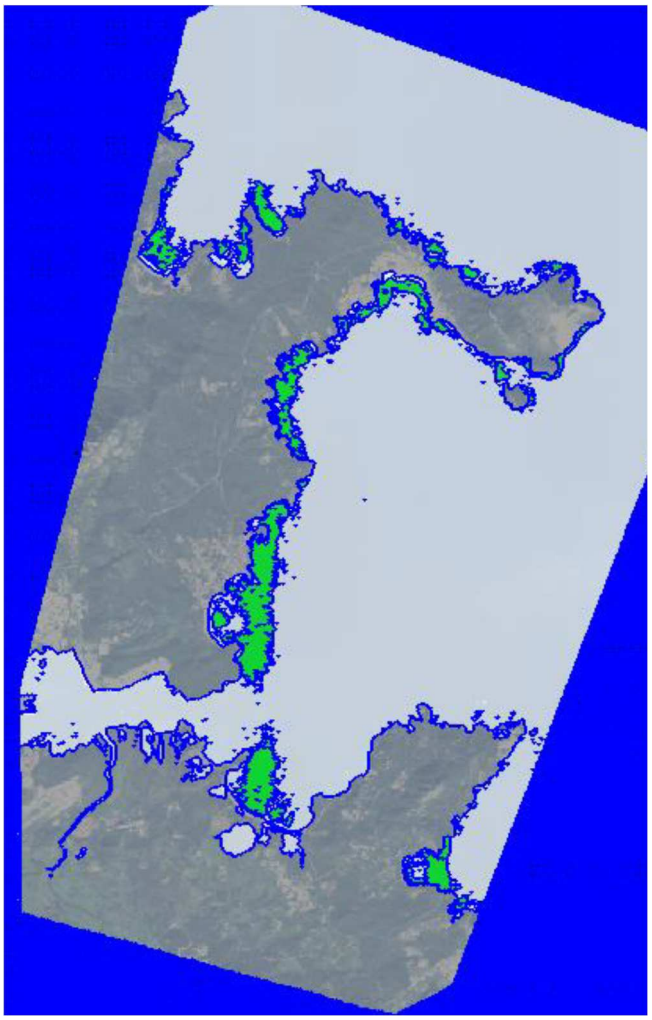

Fig. 4. Result of object-based classification of the multispectral image of the year 2021 with bathymetric correction. In dark grey the land, in light grey the sea, in green the *P. oceanica.*

CONCLUSIONS

This study highlights the potential of high-resolution satellite imagery and classification tools for mapping *P. oceanica* meadows. While the absence of marine control points remains a challenge, applying bathymetric correction improved overall geometric accuracy and led to more consistent results between pixel-based and object-based classification. However, this should be considered a preliminary assessment, and further tests on different areas are necessary to fully understand the causes and significance of these results.

ACKNOWLEDGMENT

The authors would like to thank Airbus DS, Sysdeco S.r.l. and Dr. Fabrizio Filiberti for their assistance and generous provision of the images Pleaides NEO © Airbus DS (acquired in year 2021, 2022) used in this study.

Authorized licensed use limited to: Universita degli Studi di Roma La Sapienza. Downloaded on December 11,2025 at 10:54:23 UTC from IEEE Xplore. Restrictions apply.

REFERENCES

[1] A. Cocozza di Montanara, F. Semprucci, F. Rendina, G. F. Russo, R. Sandulli, "Re-discovering macerating Posidonia oceanica bottoms: Characterization of meiofaunal community inhabiting a peculiar Mediterranean habitat,". Estuarine, Coastal and Shelf Science, 309, 108956, 2024, https://doi.org/10.1016/j.ecss.2024.108956

[2] L. Telesca, A. Belluscio, A. Criscoli, G. Ardizzone, E. T. Apostolaki, S., Fraschetti, M. Gristina, L. Knittweis, C. S. Martin, G. Pergent, A. Alagna, F. Badalamenti, G. Garofalo, V. Gerakaris, M. Louise Pace, C. Pergent-Martini, M. Salomidi, "Seagrass meadows (Posidonia oceanica) distribution and trajectories of change," Scientific Reports, 5, 1–14, 2015, https://doi.org/10.1038/srep12505

[3] F. Blanco-Murillo, S. Jimenez-Gutierrez, J. Martínez-Vidal, J. E. Guillén, J. L. Sánchez-Lizaso, "Spatiotemporal Trends Observed in 20 Years of Posidonia oceanica Monitoring along the Alicante Coast, Spain," Water (Switzerland), 14(3), 1–11, 2022 https://doi.org/10.3390/w14030274

[4] S. M. Trevathan-Tackett, J. Kelleway, P. I. Macreadie, J. Beardall, P. Ralph, and A. Bellgrove, "Comparison of marine macrophytes for their contributions to blue carbon sequestration," 96: 3043-3057, 2015 https://doi.org/10.1890/15-0149.1

[5] D. Trogu, S. Simeone, A. Ruju, M. Porta, A. Ibba, S. DeMuro, "A Four-Year Video Monitoring Analysis of the Posidonia oceanica Banquette Dynamic: A Case Study from an Urban Microtidal Mediterranean Beach (Poetto Beach, Southern Sardinia, Italy)," Journal of Marine Science and Engineering, 11(12), 2023, https://doi.org/10.3390/jmse11122376

[6] "Posidonia oceanica e pesca professionale", AGCI Agrital, Settore Agro Ittico Alimentare Programmazione Piano Nazionale Pesca 2019. https://www.agciagrital.it/wp-content/uploads/2019/10/Posidonia-e-pesca_compressed.pdf last visited: 02 May 2025

[7] C. Robello, S. Acunto, L. M. Leone, I. Mancini, A. Oprandi, M. Montefalcone "Large-Scale Re-Implantation Efforts for Posidonia oceanica Restoration in the Ligurian Sea: Progress and Challenges," Diversity, 16, 226, 2024, https://doi.org/10.3390/d16040226

[8] A. A. Peru, F. Susana, A.M.L. Carlos, E. H. Iris, "Water column oxygenation by Posidonia oceanica seagrass meadows in coastal areas: A modelling approach," Science of The Total Environment, Volume 942, 173805, 2024, https://doi.org/10.1016/j.scitotenv.2024.173805

[9] D. Ventura, A. Bonifazi, M. F. Gravina, A. Belluscio, G. Ardizzone "Mapping and classification of ecologically sensitive marine habitats using unmanned aerial vehicle (UAV) imagery and Object-Based Image Analysis (OBIA)," Remote Sensing, 10(9), 1–23, 2018, https://doi.org/10.3390/rs10091331

[10] V. Baiocchi, F. Zottele, D. Dominici, "Remote sensing of urban microclimate change in L'Aquila city (Italy) after post-earthquake depopulation in an open source GIS environment," Sensors (Switzerland), Volume 17, Issue 219, Article number 404, 2017, https://doi.org/0.3390/s17020404

[11] V. Baiocchi, F. Cianfanelli, E. Nocerino, "Satellite Images and Bathymetric LiDAR for Mapping Seagrass Meadows: An Overview" In Earth Observation: Current Challenges and Opportunities for Environmental Monitoring; AIT Series. Trends in Earth Observation; Associazione Italiana di Telerilevamento: Firenze, Italy, Volume 3, pp. 87–92, 2024

[12] C. Cocozza, A. Parente, C. Zaccone, C. Mininni, P. Santamaria, P.; T. Miano, "Comparative management of offshore posidonia residues: Composting vs. energy recovery" Waste Manag., 31, pp. 78–84, 2011

[13] C. Parente, E. Alcaras, f. g. Figliomeni, "Coastline Automatic Extraction from Medium-Resolution Satellite Images Using Principal Component Analysis (PCA)-Based Approach," Remote Sens. , 16, 1817, 2024, https://doi.org/10.3390/rs16101817

[14] G. Ceccherelli, F. Chiabrando, F. Gallitto, A. Lingua, A., V. Longhi, P. Maschio, F. Matrone, F. Menna, E. Nocerino, M. Scalici, et al., "Multitemporal Seagrass Mapping and Monitoring of Posidonia Meadows and Banquettes for Blue Carbon Conservation: The Poseidon Project," Int. Arch. Photogramm. Remote Sens. Spat. Inf. Sci., 48, 65–71, 2024.

[15] M. Chowdhury, A. Martínez-Sansigre, M. Mole, E. Alonso-Peleato, N.o Basos, J. M. Blanco, M. Ramirez-Nicolas, I. Caballero, I., de la Calle Perez, "AI-driven remote sensing enhances Mediterranean seagrass monitoring and conservation to combat climate change and anthropogenic impacts," Scientific Reports. 14, 2024 https://doi.org/10.1038/s41598-024-59091-7

[16] C. B. Khan, K. T. Goetz, H. C. Cubaynes, C. Robinson, E. Murnane, T. Aldrich, M. Sackett, P. J. Clarke, M. A. LaRue, T. White, K. Leonard, A. Ortiz, J. M. Lavista Ferres, "Biologist's Guide to the Galaxy: Leveraging Artificial Intelligence and Very High-Resolution Satellite Imagery to Monitor Marine Mammals from Space," J. Mar. Sci. Eng. 11, 595, 2023, https://doi.org/10.3390/jmse11030595

[17] S. Mohanty, P. K. Srivastava, P. C. Pandey, P. Singh, S. Srivastava, "Wetland species mapping using advanced technological measurement," Aquatic Conservation: Marine and Freshwater Ecosystems, 2024, https://doi.org/10.1002/aqc.70018

Authorized licensed use limited to: Universita degli Studi di Roma La Sapienza. Downloaded on December 11,2025 at 10:54:23 UTC from IEEE Xplore. Restrictions apply.